

Determination of the high pressure phases of CaWO_4 by CALYPSO and X-ray diffraction studies

HPSTAR
307_2016

Li Wang¹, Feng Ke², Yuwei Li¹, Qinglin Wang³, Cailong Liu¹, Jiejuan Yan¹, Hui Li¹, Yonghao Han^{*1}, Yanzhang Ma^{2,4}, and Chunxiao Gao^{**1}

¹ State Key Laboratory of Superhard Materials, Institute of Atomic and Molecular Physics, Jilin University, Changchun 130012, P.R. China

² Center for High Pressure Science and Technology Advanced Research, Shanghai 201203, P.R. China

³ Shandong Key Laboratory of Optical Communication Science and Technology, School of Physics Science & Information Technology, Liaocheng University, Liaocheng 252059, P.R. China

⁴ Department of Mechanical Engineering, Texas Tech University, Lubbock, TX 79409, USA

Received 5 April 2016, revised 16 May 2016, accepted 8 June 2016

Published online 24 June 2016

Keywords CALYPSO, CaWO_4 , crystal structure, high pressure, phase transition, X-ray diffraction

* Corresponding author: e-mail hanyh@jlu.edu.cn, Phone: +86 431 516 8878 601, Fax: +86 431 516 8878 602

** e-mail cc060109@qq.com, Phone: +86 431 516 8878 601, Fax: +86 431 516 8878 602

Theoretical and experimental methods have been conducted to study the high-pressure structures of CaWO_4 , which have never been definitely determined during the past decades. By using the CALYPSO method, in addition to the previously known tetragonal scheelite structure ($I4_1/a$), monoclinic fergusonite structure ($I2/a$), and the orthorhombic structure ($Cmca$) predicted by previous works, we have found two other new phases of CaWO_4

at higher pressure: monoclinic $P2_1/c$ and $P2_1/m$ structures. Although the $P2_1/c$ structure has the lowest energy (above 26.0 GPa), synchrotron-radiation-based X-ray diffraction measurements show that only the $P2_1/m$ structure stably exists above 38.0 GPa. The kinetical hindrance of $P2_1/c$ structure formation in the experiment has been attributed to its larger W-O coordination number than that of the $P2_1/m$ structure at high pressure.

© 2016 WILEY-VCH Verlag GmbH & Co. KGaA, Weinheim

1 Introduction The study of the structures of scheelite (CaWO_4) under high pressure is interesting because these structures have never been definitely determined in past decades through various theoretical and experimental approaches, including first-principles calculations, Raman spectra, and X-ray diffraction (XRD) measurements.

Scheelite is a naturally formed mineral. High-pressure structural studies of CaWO_4 are significant for understanding the layer distribution of scheelite deposits in the earth. Many other ABO_4 compounds, such as CaMoO_4 , PbWO_4 , and the high pressure phase of zircon, are also isostructural to CaWO_4 [1]; therefore, relevant structural studies of CaWO_4 at high pressure can provide valuable references for the determination of the phase transitions of those isostructural materials.

Under ambient conditions, CaWO_4 crystallizes into a tetragonal structure with $I4_1/a$ symmetry. From XRD

measurements [2], Grzechnik et al. found that CaWO_4 transforms from the tetragonal scheelite structure to the monoclinic fergusonite structure ($I2/a$) at ~ 10.0 GPa, which was further confirmed by other XRD measurements [3–5] and *ab initio* calculations [4, 5]. With further compression, Botella et al. recently found another structural phase transition at ~ 34.4 GPa by using the Raman spectroscopic method [6]; the new phase was identified as having an orthorhombic structure with $Cmca$ symmetry via first-principles calculations [5, 6]. However, Goel et al. proposed that CaWO_4 would be amorphous at ~ 32.0 GPa according to molecular dynamics simulations [7], and Errandonea et al. obtained a similar result at ~ 40.0 GPa via energy dispersive XRD measurements [8]. Previous studies of CaWO_4 at high pressure have essentially reached an agreement regarding the structure determination before and after the phase transition at ~ 10.0 GPa, but the

high-pressure structure after the phase transition between 32.0 and 40.0 GPa has not been definitely determined. Moreover, whether new structures would emerge at higher pressures is another interesting issue.

Motivated by the above-mentioned issues, in this paper, we used the crystal structure analysis by particle swarm optimization (CALYPSO) method [9, 10] and synchrotron-radiation-based high-pressure XRD measurements to study the structural properties of CaWO₄ at high pressures. We found that CaWO₄ transformed from *I*4₁/*a* phase to *I*2/*a* phase at ~10.0 GPa, and then to layered monoclinic structure (*P*2₁/*m*) at ~38.0 GPa.

2 Methods

2.1 Computational details

CALYPSO is an efficient and accurate method for determining the structures of materials under given conditions [11–14]. *Ab initio* structural relaxation and electronic structure calculations were carried out by using density functional theory with the Perdew–Burke–Ernzerh (PBE) generalized gradient approximation [15] exchange–correlation potential, as implemented in the VASP code [16]. The projector augmented wave (PAW) method [17] was adopted, with 3p⁶4s², 5p⁶6s²5d⁴, and 2s²2p⁴ electrons as valences for Ca, W, and O, respectively. An energy cutoff of 520 eV for the plane-wave expansion and a Brillouin zone integration grid spacing of $2\pi \times 0.037 \text{ \AA}^{-1}$ produced enthalpy results that well converged. To examine the dynamic stability of the new high pressure phases, we calculated the phonon dispersion by using the PHONOPY code [18]. The energy bands were calculated by using the Heyd–Scuseria–Ernzerhof (HSE06) screened hybrid functional [19, 20].

2.2 Experimental details

High-pressure XRD measurements were performed at beamline 4W2 of the Beijing Synchrotron Radiation Facility and 15U1 of the Shanghai Synchrotron Radiation Facility ($\lambda = 0.6199 \text{ \AA}$). CaWO₄ powder with a purity of 99.78%, bought from the Alfa Aesar Company, was loaded into a diamond anvil cell with a culet of 300 μm in diameter. Silicone oil and liquid argon were used as the pressure-transmitting media, respectively. Pressure was calibrated by using the R1 fluorescence peak of ruby [21]. Diffraction images were integrated with FIT2D software to obtain intensity versus 2θ patterns [22]. Rietveld refinements were carried out using the GSAS program [23].

3 Results and discussion

Structure predictions were performed in the pressure range of 0–60 GPa by using the CALYPSO code with four formula units per simulation cell. The CALYPSO method can successfully predict the tetragonal *I*4₁/*a* structure at ambient pressure and monoclinic *I*2/*a* structure (Fig. 1(a)) at 15 GPa, validating its high reliability in the prediction of high-pressure structures. At 50 GPa, in addition, the orthorhombic *Cmca* structure predicted by previous works [5, 6], we also found a

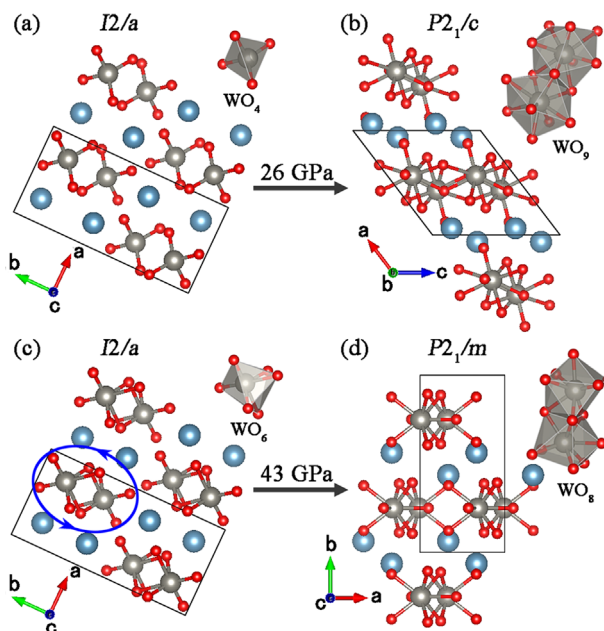


Figure 1 Crystal structures of CaWO₄: (a), (c) *I*2/*a* phase, (b) *P*2₁/*c* phase, and (d) *P*2₁/*m* phase. The blue, gray, and red spheres indicate Ca, W, and O atoms, respectively. The 26 and 43 GPa are the calculated transition pressures. The arrows on the blue ellipse represent the rotation direction of the zigzag chains in the phase transition process.

monoclinic *P*2₁/*c* structure and a monoclinic *P*2₁/*m* structure, as shown in Fig. 1(b) and (d), respectively. The structural information of *P*2₁/*c* and *P*2₁/*m* phases is summarized in Table 1.

We calculated enthalpy curves of the predicted phases (see Supporting Information (SI), Fig. S1). As shown in Fig. S1, the calculated transition pressures of *I*2/*a*-to-*Cmca*,

Table 1 Structural parameters of the predicted *P*2₁/*c* and *P*2₁/*m* phases.

lattice params	atoms	<i>x</i>	<i>y</i>	<i>z</i>
<i>P</i> 2 ₁ / <i>c</i> 40 GPa: <i>a</i> = 7.259 \AA <i>b</i> = 5.307 \AA <i>c</i> = 7.307 \AA β = 129.266°	Ca (4e)	0.0622	0.7466	0.6815
	W (4e)	0.4377	0.2095	0.7927
	O (4e)	0.6783	0.4836	0.9772
	O (4e)	0.8656	0.6676	0.8048
	O (4e)	0.2609	0.9890	0.0905
	O (4e)	0.4354	0.8364	0.8799
<i>P</i> 2 ₁ / <i>m</i> 50 GPa: <i>a</i> = 5.184 \AA <i>b</i> = 9.589 \AA <i>c</i> = 4.940 \AA β = 61.887°	Ca (4f)	0.6682	0.5640	0.6664
	W (2e)	0.3201	0.7500	0.3283
	W (2e)	0.9888	0.2500	0.0177
	O (4f)	0.2473	0.8871	0.6514
	O (4f)	0.0903	0.8928	0.2270
	O (4f)	0.3355	0.3766	0.8351
	O (2e)	0.4291	0.7500	0.8982
	O (2e)	0.9012	0.7500	0.6595

$I2/a$ -to- $P2_1/c$ and $I2/a$ -to- $P2_1/m$ phase transitions are about 27, 26, and 43 GPa, respectively. Above 26 GPa, the $P2_1/c$ structure was found to have the lowest energy. To verify the dynamic stability of the $P2_1/c$ and $P2_1/m$ phases, we calculated the phonon dispersion curves (see SI, Fig. S2). There were no imaginary phonon modes in the whole Brillouin zone, indicating that the $P2_1/c$ and $P2_1/m$ phases are dynamically stable.

We have subsequently performed high-pressure XRD experiments up to 53.8 GPa. Selected XRD patterns of CaWO_4 , with silicone oil and liquid argon as the pressure-transmitting media, are shown in Figs. 2 and 3, respectively. All diffraction patterns below 8.7 GPa in Fig. 2 or 11.2 GPa in Fig. 3 can be well indexed to the tetragonal scheelite structure ($I4_1/a$). Above 8.7 or 11.2 GPa, several new peaks can be observed, clearly indicating a pressure-induced phase transition. The result of Rietveld refinement indicates that the XRD patterns of the high pressure phase can be refined precisely with the monoclinic fergusonite structure in $I2/a$

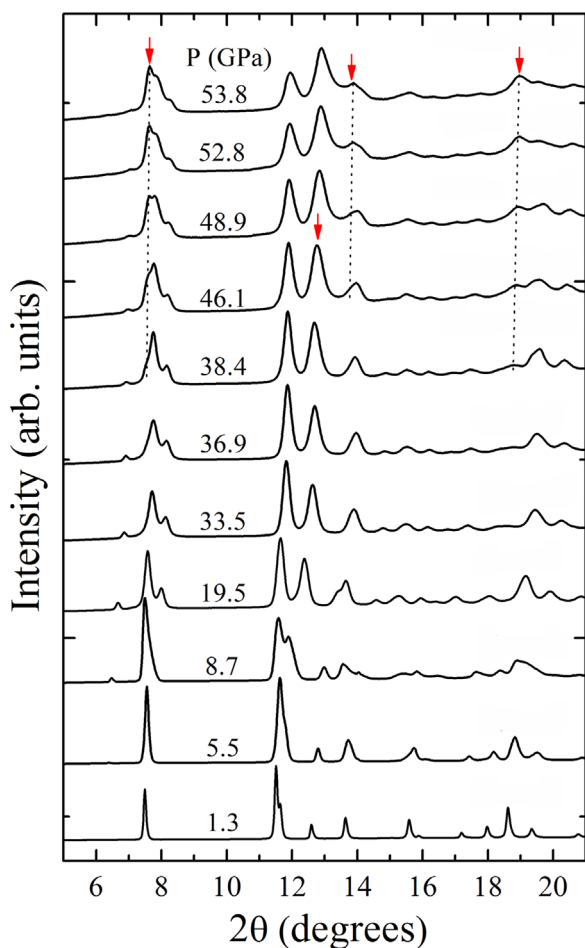


Figure 2 Selected XRD patterns of CaWO_4 with silicone oil as the pressure-transmitting medium. The peaks marked as arrows and dotted lines are the diffraction peaks of the new high pressure phase above ~ 38.0 GPa.

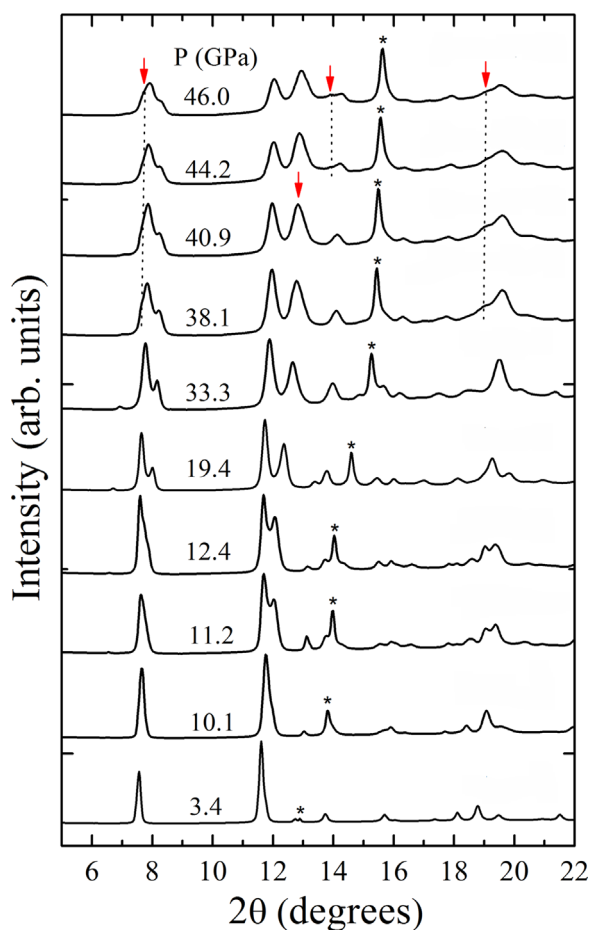


Figure 3 Selected XRD patterns of CaWO_4 with liquid argon as the pressure-transmitting medium. The peaks marked as arrows and dotted lines are the diffraction peaks of the new high pressure phase above ~ 38.0 GPa. The asterisks indicate the liquid argon diffraction peaks.

symmetry, as shown in Fig. 4(b), consistent with the previously reported observations [2–5]. According to the Rietveld refinements (see Fig. 4(a) and (b)), the unit cell parameters of the $I4_1/a$ phase at 1.3 GPa and $I2/a$ phase at 19.5 GPa are $a = 5.211 \text{ \AA}$, $c = 11.282 \text{ \AA}$, and $a = 5.225 \text{ \AA}$, $b = 10.599 \text{ \AA}$, $c = 4.898 \text{ \AA}$, and $\beta = 95.025^\circ$, respectively. For both pressure-transmitting media, above approximately 38.0 GPa, the strength of the peak at approximately $2\theta = 12.8^\circ$ obviously increases, and three new peaks, located at $2\theta = 7.5, 13.7,$ and 18.9° , emerge, indicating that CaWO_4 transforms into a new structure and will coexist with the $I2/a$ phase up to 53.8 GPa, i.e., the highest pressure in the experiment.

Figure S3 (see SI) shows the experimental XRD data at 53.8 GPa and the simulated XRD patterns of the predicted structures at 55.0 GPa. Obviously, only the $P2_1/m$ structure is available. We refined the experimental XRD data at 53.8 GPa by using the predicted $P2_1/m$ structure and found that the new high pressure phase can be indexed to the $P2_1/m$

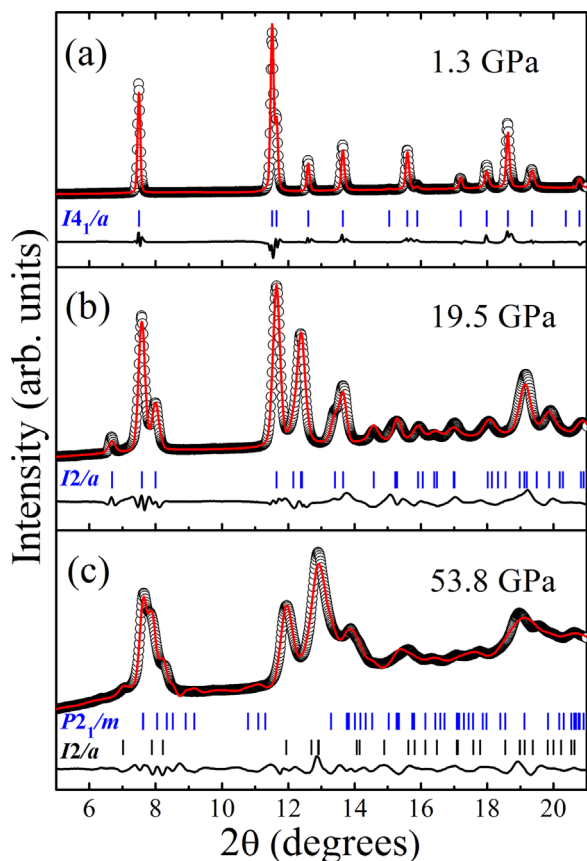


Figure 4 Rietveld refinements of the XRD patterns of CaWO_4 . The solid red lines and open circles represent the Rietveld fits and experimental data, respectively. The vertical bars indicate the peak positions, while the solid lines at the bottom are the residual intensities.

structure, as shown in Fig. 4(c). The structural parameters of the $P2_1/m$ phase at 53.8 GPa obtained by Rietveld refinement are shown in Table 2. The results of this refinement are in agreement with the structural parameters obtained from CALYPSO. The pressure dependency of the experimental volumes for the $I4_1/a$, $I2/a$, and $P2_1/m$ phases are shown in Fig. 5(a). It is obvious that the first phase

Table 2 Structural parameters of the $P2_1/m$ phase obtained by Rietveld refinement.

lattice params	atoms	x	y	z
53.8 GPa:	Ca (4f)	0.6671	0.5636	0.6678
$a = 5.181 \text{ \AA}$	W (2e)	0.3198	0.7500	0.3294
$b = 9.321 \text{ \AA}$	W (2e)	0.9906	0.2500	0.0155
$c = 4.903 \text{ \AA}$	O (4f)	0.2444	0.8879	0.6539
$\beta = 63.217^\circ$	O (4f)	0.0905	0.8939	0.2265
	O (4f)	0.3361	0.3771	0.8333
	O (2e)	0.4289	0.7500	0.8977
	O (2e)	0.9000	0.7500	0.6592

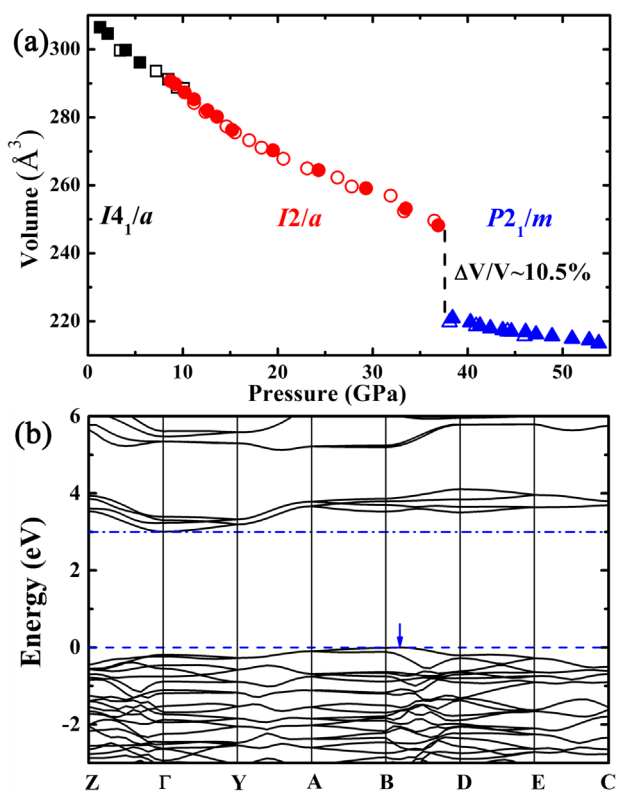


Figure 5 (a) Experimental volumes as a function of pressure for different phases. Solid and open symbols refer to data with silicone oil and liquid argon as the pressure-transmitting media, respectively. (b) Electronic band structure of $P2_1/m$ phase at 45 GPa. The VBM and CBM are denoted by a dashed line and a dot-dashed line, respectively.

transition can be classified as a second-order phase transition without a discontinuous volume change; the second phase transition can be characterized by a first-order transition accompanying an $\sim 10.5\%$ volume drop.

Surprisingly, the $P2_1/c$ structure in the calculations has the lowest energy above 26.0 GPa, but in our experiments, CaWO_4 still transforms directly from $I2/a$ to $P2_1/m$ at ~ 38.0 GPa. Such an odd discrepancy between the theoretical calculation and experiment deserves a deep study from the viewpoint of the phase transition mechanism. Figure 1 (a) and (b) shows the simulated structural evolution from the $I2/a$ to $P2_1/c$ phase. The first-principles local optimization results show that the W^{6+} cations are fourfold coordinated by oxygens in the $I2/a$ phase below 26.0 GPa, as shown in Fig. 1(a). High pressure makes the WO_4 tetrahedral arrangement tighter and increases the stacking density. As shown in Fig. 1(b), the W^{6+} cations are ninefold coordinated by oxygens in the $P2_1/c$ structure. The $P2_1/c$ structure is a layered structure and has one CaWO_4 layer per unit cell. The phase transition route from $I2/a$ to $P2_1/m$ is shown in Fig. 1(c) and (d). The coordination number of W^{6+} cations is six in the $I2/a$ phase above 36.0 GPa, and the structure can be described with the zigzag chains of

edge-sharing WO_6 octahedrons (see SI, Fig. S4). At 43.0 GPa, the pressure forces the zigzag chains to rotate (as indicated by the arrows in Fig. 1(c)) and connect to each other; eventually, the $I2/a$ structure transforms into the $P2_1/m$ structure, with a larger coordination number up to eight, as shown in Fig. 1(d). The $P2_1/m$ structure can be viewed as the stacks of a - c layers along the b axis. It has two centrosymmetric CaWO_4 layers per unit cell.

Therefore, it is clear that the W–O coordination number of the $P2_1/c$ structure is larger than that of the $P2_1/m$ structure, leading to a denser atomic arrangement in the $P2_1/c$ structure and a higher energy barrier for the phase transition from $I2/a$ to $P2_1/c$. Namely, the phase transition route is kinetically hindered [12]. However, high-temperature and high-pressure conditions might be greatly helpful in overcoming the higher energy barrier and synthesize such an intriguing $P2_1/c$ phase. Some analogous cases have been reported in the literature [12, 24].

Moreover, we calculated the electronic structure of the $P2_1/m$ phase at 45 GPa using the HSE06 hybrid function. As shown in Fig. 5(b), the $P2_1/m$ phase has a quasidirect bandgap at the Γ point; the direct bandgap is 3.20 eV. The valence band maximum (VBM) and the conduction band minimum (CBM) locate near the B point (as indicated by the blue arrow) and Γ point, respectively. Thus, the $P2_1/m$ phase has an indirect bandgap of 3.01 eV. Compared with the bandgaps of the $I4_1/a$ and $I2/a$ phases reported by previous works [25, 26], the $P2_1/m$ phase has the smallest bandgap.

4 Conclusions In summary, the high-pressure structures of CaWO_4 have been studied via a joint experimental and theoretical study. By using structure prediction via the CALYPSO method, we predicted two new high pressure phases having the monoclinic $P2_1/c$ and $P2_1/m$ structures. However, synchrotron-radiation-based X-ray diffraction measurements showed that only the monoclinic $P2_1/m$ structure stably exists above 38.0 GPa. We attribute the $P2_1/c$ structure to a high-temperature, high pressure phase. This work observes the $I2/a$ -to- $P2_1/m$ phase transition for the first time in an X-ray diffraction experiment and enriches the information regarding ABO_4 compounds under high pressure. It is an important reference for the high-pressure research of other ABO_4 compounds.

Supporting Information Additional supporting information may be found in the online version of this article at the publisher's web-site.

Acknowledgements This work was supported by the National Natural Science Foundation of China (grant nos. 11374121 and 11404133) and the Program of Science and Technology Development Plan of Jilin Province (grant no. 20140520105JH).

References

- [1] D. Errandonea and F. J. Manjón, *Prog. Mater. Sci.* **53**, 711 (2008).
- [2] A. Grzechnik, W. A. Crichton, M. Hanfland, and S. v. Smaalen, *J. Phys.: Condens. Matter* **15**, 7261 (2003).
- [3] R. Vilaplana, R. Lacomba-Perales, O. Gomis, D. Errandonea, and Y. Meng, *Solid State Sci.* **36**, 16 (2014).
- [4] P. Rodríguez-Hernández, J. López-Solano, S. Radescu, A. Mujica, A. Muñoz, D. Errandonea, J. Pellicer-Porres, A. Segura, Ch. Ferrer-Roca, F. J. Manjón, R. S. Kumar, O. Tschauner, and G. Aquilanti, *J. Phys. Chem. Solids* **67**, 2164 (2006).
- [5] D. Errandonea, J. Pellicer-Porres, F. J. Manjón, A. Segura, Ch. Ferrer-Roca, R. S. Kumar, O. Tschauner, P. Rodríguez-Hernández, J. López-Solano, S. Radescu, A. Mujica, A. Muñoz, and G. Aquilanti, *Phys. Rev. B* **72**, 174106 (2005).
- [6] P. Botella, R. Lacomba-Perales, D. Errandonea, A. Polian, P. Rodríguez-Hernández, and A. Muñoz, *Inorg. Chem.* **53**, 9729 (2014).
- [7] P. Goel, M. K. Gupta, R. Mittal, S. Rols, S. N. Achary, A. K. Tyagi, and S. L. Chaplot, *Phys. Rev. B* **91**, 094304 (2015).
- [8] D. Errandonea, M. Somayazulu, and D. Häusermann, *Phys. Status Solidi B* **235**, 162 (2003).
- [9] Y. C. Wang, J. Lv, L. Zhu, and Y. M. Ma, *Phys. Rev. B* **82**, 094116 (2010).
- [10] Y. C. Wang, J. Lv, L. Zhu, and Y. M. Ma, *Comput. Phys. Commun.* **183**, 2063 (2012).
- [11] Y. W. Li, Y. C. Wang, C. J. Pickard, R. J. Needs, Y. Wang, and Y. M. Ma, *Phys. Rev. Lett.* **114**, 125501 (2015).
- [12] G. T. Liu, L. Zhu, Y. M. Ma, C. L. Lin, J. Liu, and Y. M. Ma, *J. Phys. Chem. C* **117**, 10045 (2013).
- [13] F. Peng, M. S. Miao, H. Wang, Q. Li, and Y. M. Ma, *J. Am. Chem. Soc.* **134**, 18599 (2012).
- [14] Y. C. Wang, H. Y. Liu, J. Lv, L. Zhu, H. Wang, and Y. M. Ma, *Nature Commun.* **2**, 563 (2011).
- [15] J. P. Perdew, K. Burke, and M. Ernzerhof, *Phys. Rev. Lett.* **77**, 3865 (1996).
- [16] G. Kresse and J. Furthmüller, *Phys. Rev. B* **54**, 11169 (1996).
- [17] G. Kresse and D. Joubert, *Phys. Rev. B* **59**, 1758 (1999).
- [18] A. Togo, F. Oba, and I. Tanaka, *Phys. Rev. B* **78**, 134106 (2008).
- [19] A. V. Krukau, O. A. Vydrov, A. F. Izmaylov, and G. E. Scuseria, *J. Chem. Phys.* **125**, 224106 (2006).
- [20] J. Heyd, G. E. Scuseria, and M. Ernzerhof, *J. Chem. Phys.* **118**, 8207 (2003).
- [21] H. K. Mao, P. M. Bell, J. W. Shaner, and D. J. Steinberg, *J. Appl. Phys.* **49**, 3276 (1978).
- [22] A. P. Hammersley, S. O. Svensson, M. Hanfland, A. N. Fitch and D. Häusermann, *High Press. Res.* **14**, 235 (1996).
- [23] B. H. Toby, *J. Appl. Crystallogr.* **34**, 210 (2001).
- [24] E. Y. Atabaeva, S. A. Mashkov, and S. V. Popova, *Kristallografiya* **18**, 173 (1973).
- [25] R. Lacomba-Perales, J. Ruiz-Fuertes, D. Errandonea, D. Martínez-García, and A. Segura, *Europhys. Lett.* **83**, 37002 (2008).
- [26] R. Lacomba-Perales, D. Errandonea, A. Segura, J. Ruiz-Fuertes, P. Rodríguez-Hernández, S. Radescu, J. López-Solano, A. Mujica, and A. Muñoz, *J. Appl. Phys.* **110**, 043703 (2011).